

Airbrushing: A Novel Method for Preparation of High-Emissivity Black Coating for Infrared Measurements

Victor Regis, Geoff Brennecka, Urban Tomc, Andrej Kitanovski, Jan Cerar, Jaka Tušek, Ivan Jerman, Enric Stern-Taulats, Klara Lünser, Lluís Mañosa, and Hana Uršič*

The reliability of infrared (IR) imaging is strongly dependent on the surface emissivity of the investigated object. Achieving near-unity emissivity is essential to IR measurement accuracy. To meet this requirement, black paint coatings are commonly applied onto the studied samples. However, there is a lack of a systematic study of the coating preparation for IR measurements. In this work, a new procedure is developed for the preparation of black paint coatings using the cost-effective airbrush tool. With this novel method, it can achieve black paint coatings as thin as $\approx 3 \mu\text{m}$ or thicker, depending on the number of layers. The coatings are homogeneous and with excellent adhesion to the substrate. Furthermore, the coatings can be entirely removed from the substrate using conventional laboratory solutions. The coatings exhibited an average emissivity of ≈ 0.95 within the $0.5\text{--}2.5 \mu\text{m}$ wavelength range. The quality of the coatings is validated by directly measuring the magnetocaloric response of a commercially available material, which is in excellent agreement with the supplier's datasheet. In this way, a novel affordable black coating method is showcased, which can be applied on a wide variety of samples for IR measurements, broadening the possibilities for IR characterizations.

science, relevant properties are typically studied at temperatures a few hundred degrees below or above room temperature (near room temperature conditions).^[2,3] At these conditions, most of the emitted radiation will exhibit a wavelength between 750 nm and $\approx 50 \mu\text{m}$, within the infrared (IR) spectrum.^[2] In light of this, the IR camera method of imaging was developed allowing for real-time heat maps, or thermographs, of a wide variety of objects and has been used in several research fields.^[4–7] In biology, for example, IR imaging is used to investigate the heat dissipation mechanisms in different species of plants and animals,^[8–10] and in human medicine, as an early-stage indication of illness.^[11–13] In the research of inorganic materials, IR thermal camera imaging has been used to investigate the structural, microstructural, electrical or magnetic properties.^[14–18] A key

parameter to ensure the reliability and accuracy of IR imaging is emissivity, which is defined as the effectiveness of a surface in emitting thermal radiation. The closer it is to unity, the more the surface behaves as an ideal black-body.^[5–7] In organic tissues, the emissivity was shown to be between 0.7 and 0.95 ,^[8–13] while metals can exhibit emissivities as low as 0.02 or as high as 0.6 , depending on the material, surface conditions, and preparation methods.^[19–25] Generally, low-emissivity surfaces, such as metals

1. Introduction

Any material whose temperature is above absolute zero radiates energy through a process called black-body emission, which, according to Planck's law, encompasses the entire electromagnetic spectrum. In nature, the temperatures of objects vary significantly, for example, in astronomy, objects of interest, such as stars, can exceed 5000 Kelvin ,^[1] whereas in biology and materials

V. Regis, H. Uršič
Electronic Ceramics Department
Jožef Stefan Institute
Jamova cesta 39, Ljubljana 1000, Slovenia
E-mail: hana.ursic@ijs.si

V. Regis, H. Uršič
Jožef Stefan International Postgraduate School
Jamova cesta 39, Ljubljana 1000, Slovenia

G. Brennecka
Colorado School of Mines
1500 Illinois Ave., Golden, CO 80401, USA

U. Tomc, A. Kitanovski, J. Cerar, J. Tušek
Faculty of Mechanical Engineering
University of Ljubljana
Aškerceva cesta 6, Ljubljana 1000, Slovenia

I. Jerman
Laboratory for Coating Development
Department of Materials Chemistry
National Institute of Chemistry
Hajdrihova 19, Ljubljana 1000, Slovenia
E. Stern-Taulats, K. Lünser, L. Mañosa
Departament de Física de la Matèria Condensada
Facultat de Física
Martí i Franquès 1
Universitat de Barcelona
Barcelona 08028, Catalonia, Spain

 The ORCID identification number(s) for the author(s) of this article can be found under <https://doi.org/10.1002/admi.202500467>

© 2025 The Author(s). Advanced Materials Interfaces published by Wiley-VCH GmbH. This is an open access article under the terms of the [Creative Commons Attribution](#) License, which permits use, distribution and reproduction in any medium, provided the original work is properly cited.

DOI: 10.1002/admi.202500467

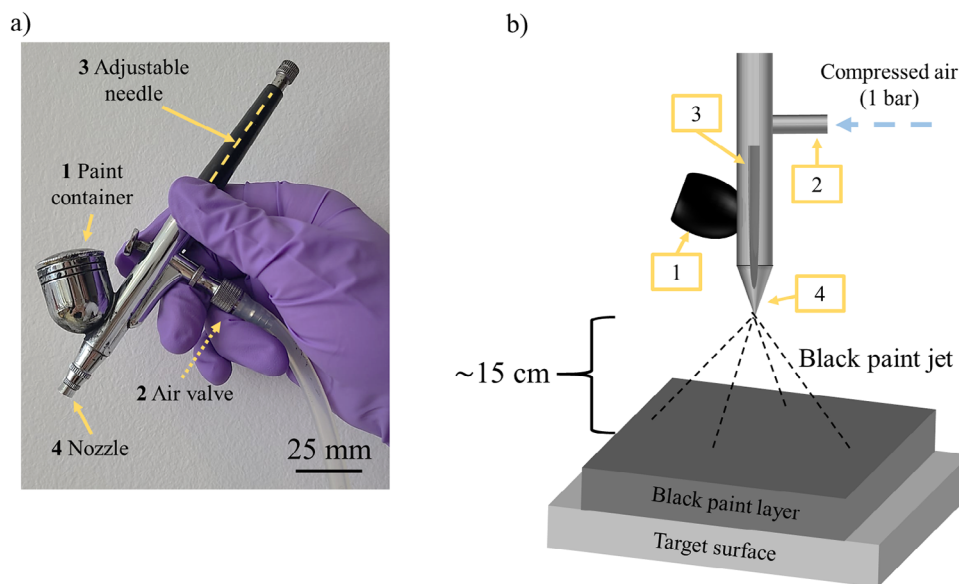


Figure 1. a) Photograph of the airbrush used in this work. b) Schematic representation of coating procedure. The numbered labels indicate the same components of the airbrush.

and ceramics, will be coated with black paint to ensure a high emissivity during the IR thermal camera investigations.^[14–19,26–31]

In recent years, there has been an increase in studies on materials that exhibit an adiabatic and reversible temperature change as a response to an electric field, magnetic field, uniaxial stress or hydrostatic pressure, namely the electrocaloric, magnetocaloric, elastocaloric or barocaloric effect, respectively.^[32–38] In the case of conventional caloric materials, when an external stimulus is applied, in isothermal conditions, the entropy in the material will decrease, which, in adiabatic conditions, will lead to an increase in temperature. After thermal relaxation, the material will return to ambient temperature, and the removal of the stimulus will result in a decrease in temperature, which can potentially be used to cool down the target object. Caloric technology is a cleaner and potentially more energy-efficient alternative to traditional vapor-compression cooling and is often integrated into active regenerators to enhance performance and minimize thermal losses.^[33,34] However, despite their promising properties, current prototypes cannot yet compete with commercial cooling systems due to various limitations. Incorporating thermal control devices, such as thermal diodes and switches, can further reduce these drawbacks and improve the efficiency of caloric-based systems.^[39,40] In the search for better caloric materials, the IR method has been widely used to characterize the thermal output of materials,^[16–18,29,41] as this method is contactless and therefore minimizes thermal losses during the measurements. However, most magnetocaloric and elastocaloric materials are metals or alloys, in addition electrocaloric materials require metal electrodes for applications of electric fields, producing surfaces with very low emissivity. To circumvent such issue, prior to the IR measurements, the surface of the materials is coated with a high emissivity coating, usually black paint. However, in most research articles, the coating procedure is often not detailed.^[42–47] To the authors' knowledge, researchers typically use spray painting techniques with commercially available paints to produce the black coatings. This

method lacks control over the thickness, homogeneity and roughness of the coating. As a result, the coating can be as thick as $\approx 100\ \mu\text{m}$.^[48,49] Evidently, this method is unsuitable for samples with a thickness lower than $100\ \mu\text{m}$, as the paint will act as a significant heat sink, which significantly affects the temperature measurements in the caloric system. Recently, there were two reports^[16,17] on IR imaging of $3\text{-}\mu\text{m}$ -thick electrocaloric films, where the authors systematically produced $\approx 3.5\ \mu\text{m}$ coatings of conventional black printer ink using a commercial office printer. Although the method is suitable for flexible films, the setup limits the geometry and dimension of the samples, as they must have a flat surface with no curvature or bending, and it is detrimental to brittle samples such as ceramic pellets. In light of this, a sample-geometry independent coating preparation method that can achieve controlled thickness and high emissivity is required for advanced IR thermal camera characterization.

In this work, black paint coatings were prepared using an inexpensive, easy-to-use airbrush method. This method has been previously used to prepare ceramic layers,^[50,51] but it has not yet been considered as a black coating technique for IR measurements. We propose using the airbrush method for the preparation of dense black paint coatings with $\approx 3\ \mu\text{m}$ thickness and an average emissivity of 0.95, which can be easily removed without damaging the target surfaces. In this way, we have developed a reliable, novel method for black coatings that can be used for IR camera measurements on a wide range of samples, regardless of their material, shape or size.

2. Experimental Section

The black coatings were prepared using a Filmtool Airbrush DG-30 (Filmtool, Ljubljana, Slovenia). The airbrush paint container was filled with the black-paint solution prepared from 15 mL of commercial black paint (Vallejo Primer Black, Vallejo, Barcelona, Spain) and 3 mL of paint thinner (Vallejo Airbrush

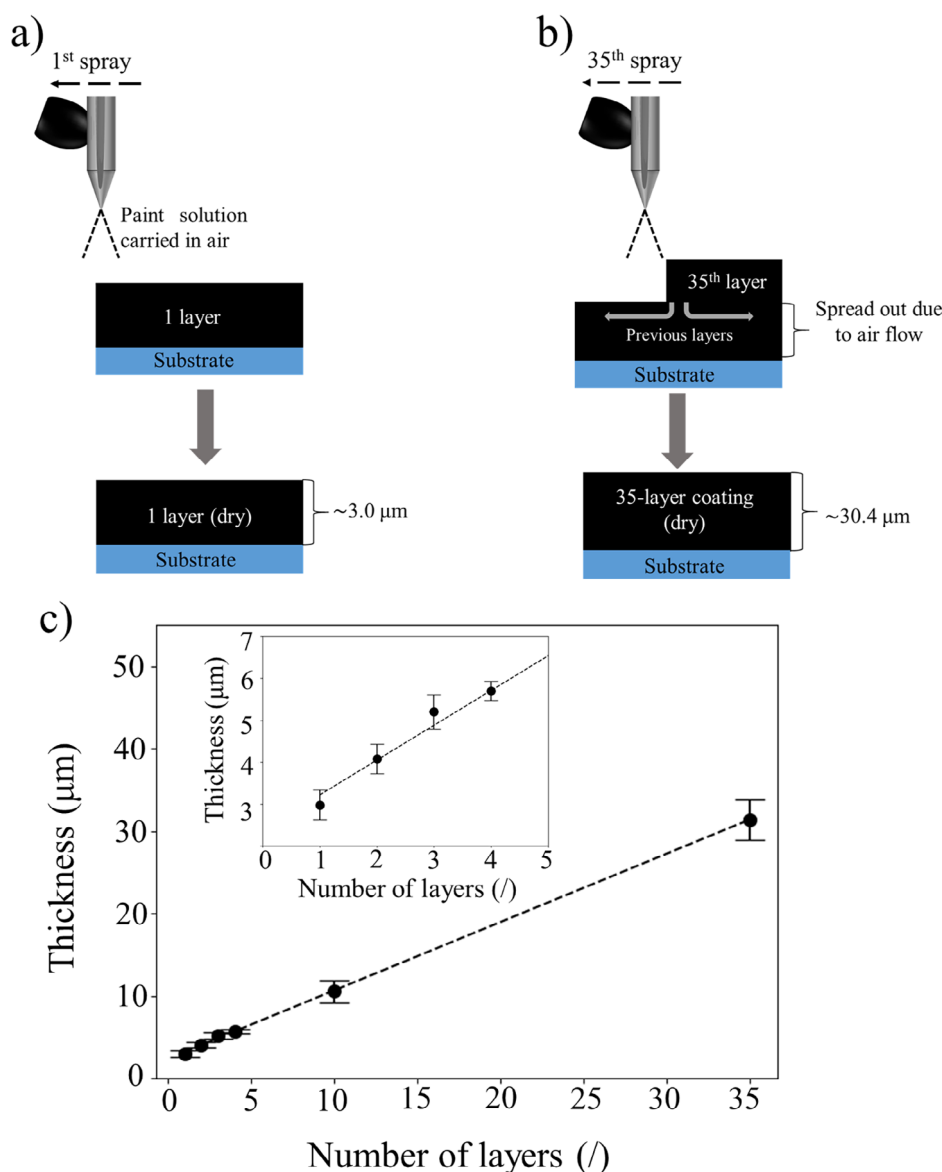


Figure 2. Schematic representation of the coating procedure for a) 1 layer and b) 35 layers. c) Average total coating thickness as a function of number of layers. The black dashed line is a guide to the eyes. The inset shows the average thickness of coatings with up to four layers.

Thinner, Vallejo, Barcelona, Spain). The airbrush can operate with a pressured difference within 0.5 and 2 bar. In this work, the compressed air was injected through the air valve at a constant pressure difference of 1 bar and regulated with the adjustable needle, as shown in Figure 1a. During the coating procedure, the airbrush nozzle was positioned 15 cm away from the target surface (Figure 1b). For the systematic investigation of the prepared coatings, 76 mm × 26 mm glass substrates (Hirschmann Labogeräte, Eberstadt, Germany) were used, which were fixed in place with conventional tape, exposing an area of ≈5 mm × 15 mm. To study the influence of the number of layers on the total thickness of the painted coatings, the substrates were painted with 1, 2, 3, 4, 10 or 35 layers of black paint. To ensure consistency, each individual layer was prepared within a time interval of ≈1 s. To reduce the influence of systematic varia-

tions between preparations, five samples were prepared for each set.

Using a contact stylus profilometer (DektakXT, Bruker, Karlsruhe, Germany) the coating thickness was measured and mean-square-root roughness (R_q) was calculated along a millimeter-long line scan. To minimize errors, the thickness and R_q measurements for each set of layers were calculated as the average of five samples. The surface and cross-section of the coatings were investigated using an optical microscope (Axio Imager M2m, Zeiss, Jena, Germany). The surface of the coatings was further investigated by atomic force microscopy (AFM; MFP-3D, Asylum Research, Santa Barbara, California, USA). Regions with the size of 80 μm × 80 μm, and 20 μm × 20 μm were scanned using titanium-iridium-coated silicon tips (Asylec-01-R2, Oxford Instruments, Abingdon, UK). The cross-sections of the samples

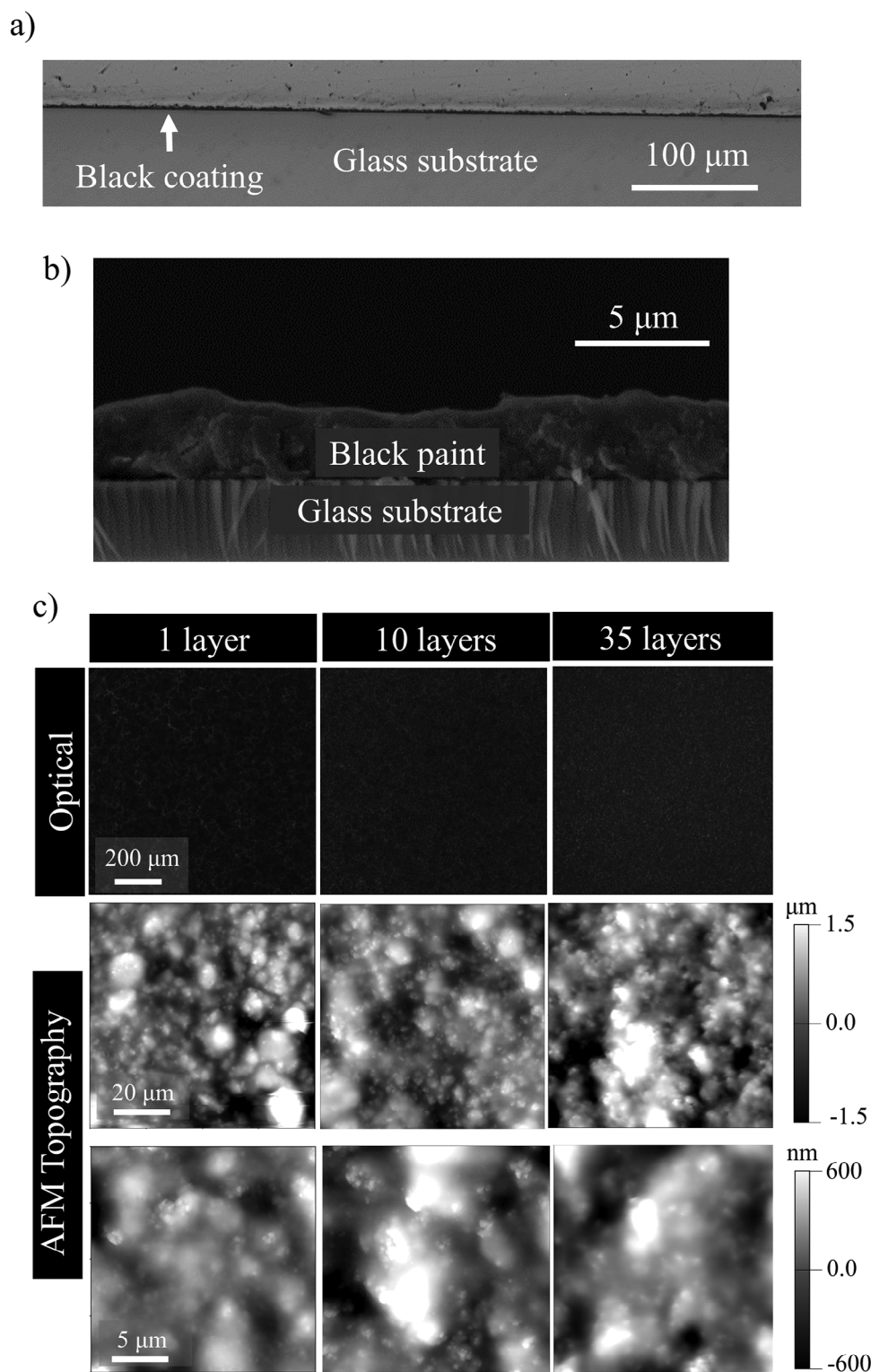


Figure 3. a) Optical microscope, and b) SEM image of single-layer coating in cross-section view. c) Optical microscope and AFM topography height images of the surface of the coatings with 1, 10, and 35 sprayed layers.

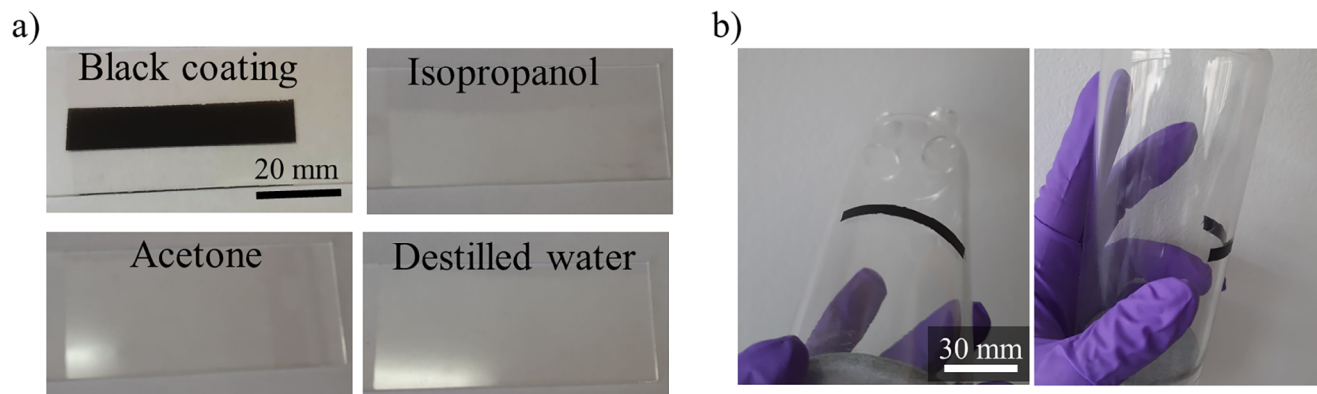


Figure 4. a) Photographs of as-prepared black coating and substrates after removal of coating using isopropanol, acetone, and distilled water. b) Photographs of single-layer on a cylindrical glass flask. Notice the pronounced curvature of the coating on the second panel.

were also investigated by scanning electron microscope (SEM; Prisma-E, Thermo Fisher, Massachusetts, USA).

For emissivity measurements, five 26 mm × 40 mm samples were coated with a single layer of black paint. The surface emissivity was characterized with the Lambda 950 spectrophotometer (Perkin Elmer, Waltham, USA), with wavelengths from 0.5 to 2.5 μm in steps of 5 nm.

For magnetocaloric measurements, 17 mm × 11 mm × 0.3 mm $\text{La}_{1.0}\text{Fe}_{10.79}\text{Si}_{1.12}\text{Co}_{1.09}$ plates (Calorivac C 292, Vacuum-schmelze GmbH & Co. KG, Hanau, Germany) were used. Prior to the coating, to remove surface contaminants, the plates were thermally treated in a chamber furnace (Custom-made, Terna, Ljubljana, Slovenia) in Argon inert atmosphere at 400 °C for 1 h with heating and cooling rates of 2 K min⁻¹. The plates were coated with a single layer under the same conditions as the glass substrates. A constant magnetic field of 1.1 T was applied using a custom-made electro-permanent magnet with a magnetization time of 10 ms.^[52,53] The measurements were done with a magnetic cycle of 50 s. Detailed information about the magnet system is provided elsewhere.^[52,53] The magnetocaloric output was characterized using an IR camera (FLIR A6750sc MWIR, FLIR,

Oregon, USA) at room temperature and with the frame rate of 100 Hz. The spectral range of the IR camera is 1–5 μm .

3. Results

During the coating process, the paint is ejected onto the target surface with air as the carrier medium. After drying, a single-layer coating achieves an average thickness of 3.0 μm schematically shown in Figure 2a. The single-layer coating is suitable for caloric characterizations, particularly of μm -thick films. However, on a general case, if the substrate roughness is large ($R_q \gg 1 \mu\text{m}$), in order to obtain reliable IR measurements, thicker coatings might be necessary. Therefore, multi-layer coatings were also prepared. As additional layers are sprayed, the incoming airflow affects the previous wet layer underneath, causing it to spread, effectively thinning the layer, while simultaneously adding more coating solution. As a result, a N -layered coating does not achieve an average thickness of $3N \mu\text{m}$. For example, a two-layer coating has an average thickness of 4.2 μm , which is lower than the expected 6.0 μm , i.e., double the single-layer thickness. At 35 layers, the average thickness reaches 30.4 μm , shown schematically in Figure 2b. It is worth emphasizing that the ratio

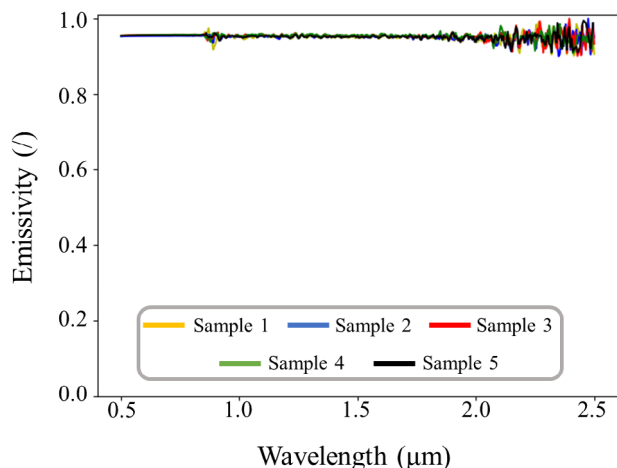


Figure 5. Emissivity of five single-layer black coatings on glass substrates. The noise at larger wavelengths can be attributed to a lower sensitivity of the detector with increasing wavelength.

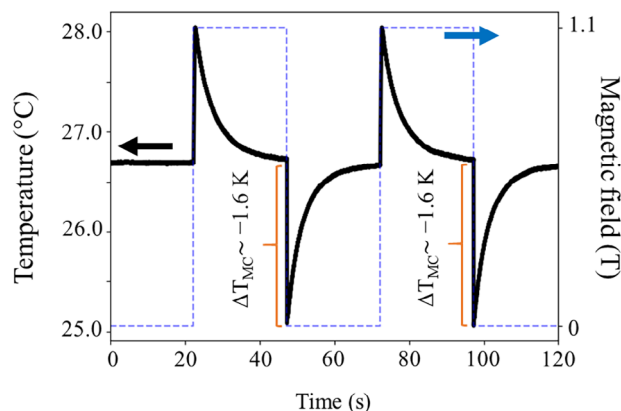


Figure 6. Temperature profile of a coated magnetocaloric plate under a cycling applied field of 1.1 T. The slight difference between heating and cooling peaks can be attributed to the difference in heat capacities of this material at zero and non-zero magnetic fields, as shown in ref. [55].

Table 1. Summary of conventional coating methods and their respective properties.

Method	Conventional spray painting ^[42–47]	Printing ^[16–18]	Airbrush (This work)
Thickness	Unreported	3.5 μm – 4.5 μm	≥ 3 μm
Samples with thickness ≥ 100 μm	✓	✗	✓
Sample with thickness < 100 μm	✗	✓	✓
Curved samples	✓	✗	✓

between the standard deviation to the average thickness in all cases is $\approx 9\%$. In addition, regardless of coating thickness, the samples exhibited comparable surface roughness within the 600 – 700 nm range, shown in Supplementary Material S1. The average total thickness as function of number of layers is shown in Figure 2c.

Single-layer coatings were investigated using optical and electron microscopes in cross-section views, as shown in Figure 3a,b. A uniform continuous coating was observed along the substrate length in both cases. Furthermore, using optical and atomic force microscopes, the surface of coatings with 1, 10, and 35 layers was investigated as shown in Figure 3c. The surface of coatings is uniform, with no visible defects, for example, porosity or pinholes, regardless of thickness.

Furthermore, the coatings are not permanent and can be easily removed from the substrates. By wiping with acetone, isopropanol or distilled water, the coatings can be completely removed without leaving any residue or damaging the substrates, shown in Figure 4a. Notably, the black paint is soluble in isopropanol and acetone, allowing for its complete removal by immersing the coated sample in the solvent. A single coating was successfully applied to a large curved glass flask, demonstrating that this method can also be applied to non-flat surfaces (Figure 4b). In addition, black paint layers can be successfully prepared on various substrates of different materials as shown in S2 (Supporting Information).

The emissivity of five single-layer coatings was characterized over the wavelength range from 0.5 to 2.5 μm , as shown in Figure 5. The coatings exhibited an average emissivity of 0.95 with a standard deviation of 0.01. Our measurements are in excellent agreement with the reported emissivity of various black paints, which are 0.92 or larger.^[16–19,28] Additional details on the emissivity measurements and the histogram distribution of the data of individual samples are provided in S3 and S4 (Supporting Information), respectively.

To investigate the suitability of the coating for IR camera measurements, the magnetocaloric plates were coated with a single layer. The IR camera used in this work covers the spectral range 1–5 μm , partially overlapping with the range (0.5–2.5 μm) of the Lambda 950 spectrophotometer used for emissivity measurements of the black coatings (more details in S5, Supporting Information). Figure 6 shows the magnetocaloric temperature change (ΔT_{MC}) of -1.60 K immediately after the field switch-off, and the same value was obtained after a second magnetic field cycle. The measurements of the magnetocaloric cooling are in accordance with the datasheet of the provider, namely -1.60 K at 1.1 T and room temperature,^[54] which confirms that the prepared black coatings are appropriate for the IR camera measurement

method. It is worth mentioning, that the value from the datasheet was obtained indirectly by measuring the magnetization at different magnetic fields and temperatures during cooling and subsequently ΔT_{MC} was calculated via the Maxwell relations.^[55] Since the black paint exhibits a very large emissivity with no significant variations within the measurement range, and the ΔT_{MC} IR measurements are in excellent agreement with the supplier's datasheet, a high emissivity can also be expected at wavelengths larger than 2.5 μm .

4. Conclusion

In this work, we investigated a non-destructive, easy-to-use coating technique for the preparation of black-paint coating for thermal camera imaging using an affordable airbrush method. The influence of the number of layers on the coating thickness was investigated, and a linearly increasing trend was observed, from an average of ≈ 3.0 μm at a single layer up to ≈ 30.4 μm at thirty-five painted layers. The coatings were homogeneous, with no visible defects and adhered well to the substrates. The surface roughness remained within 600 – 700 nm, regardless of the number of layers. The coatings were removed from the glass substrates using conventional laboratory solutions such as isopropanol, acetone and distilled water.

To demonstrate the suitability of the airbrush coating method for IR thermal camera imaging, the emissivity of the coatings was determined to be ≈ 0.95 on average. In addition, a commercially available magnetocaloric material was airbrush coated with black paint and examined using the IR imaging method under a magnetic field of 1.1 T. The measured magnetocaloric response was in excellent agreement with the literature.

In conclusion, our method enables the deposition of high-emissivity black paint coatings with thicknesses of a few microns on samples of any geometry, and combines the benefits of established techniques, such as conventional spray painting and printing as summarized in Table 1.

We propose to use the airbrush method for IR thermal imaging camera characterization of caloric bulk materials, micrometer-thick films and extend its application to other research disciplines requiring IR camera measurements.

Supporting Information

Supporting Information is available from the Wiley Online Library or from the author.

Acknowledgements

The authors acknowledge the financial support of the Slovenian Research and Innovation Agency (projects no. N2-0212 and J2-60035, program no. P2-0105, bilateral cooperation BI-US/22-24-039, BI-US/24-26-094 and young researcher project) and the transnational consortium M-ERA.NET for the project Cool BatMan: Battery Thermal Management System Based on High Power Density Digital Microfluidic Magnetocaloric Cooling (No. 9400, Slovenian part of the project was financed by the Ministry of Higher Education, Science and Innovation. Spanish part financed by MCIN/AEI/10.13039/501100011033, project No. PCI2022-132957). The Erasmus+ program is greatly acknowledged by Victor Regis. The authors also acknowledge Jena Cilenšek, Alan Selin, Val Fišinger, and Brigita Kmet for help in the laboratory, and Alexander Barcza from Vacuuschmelze GmbH, Germany, for providing the magnetocaloric samples.

Conflict of Interest

The authors declare no conflict of interest.

Data Availability Statement

The data that support the findings of this study are openly available in Zenodo at doi.org/10.5281/zenodo.15681995, reference number.^[56]

Keywords

airbrush, black paint, caloric, infrared thermal camera, IR imaging

Received: June 17, 2025

Revised: August 2, 2025

Published online: August 29, 2025

- [1] E. Bohm-Vitense, *Ann. Rev. Astron. Astrophys.* **1981**, 19, 295.
- [2] C. Meola, G. Carlomagno, *Meas. Sci. Technol.* **2004**, 15, R27.
- [3] (Ed: H. Czichos), *Handbook of Technical Diagnostics: Fundamentals and Application to Structures and Systems*, Springer Berlin, Heidelberg, Germany, **2013**.
- [4] G. Gaussorgues, *Infrared Thermography*, Springer, Dordrecht, Netherlands **1994**.
- [5] L. Ibos, M. Marchetti, A. Boudenne, S. Datcu, Y. Candau, J. Livet, *Meas. Sci. Technol.* **2006**, 17, 2950.
- [6] J. Speakman, S. Ward, *Zoology* **1998**, 101, 224.
- [7] E. Sest, G. Drazic, B. Genorio, I. Jerman, *Sol. Energy Mater. Sol. Cells* **2018**, 176, 19.
- [8] M. Jarrap, S. Rands, *Plant Methods* **2021**, 1, 17.
- [9] N. Playa-Montmanny, G. Tattersall, *Methods Ecol. Evol.* **2020**, 12, 828.
- [10] B. B. Lahiri, S. Bagavathiappan, T. Jayakumar, J. Philip, *Infrared Phys. Technol.* **2012**, 55, 221.
- [11] A. Astasio-Picadao, E. E. Martinez, A. M. Nova, R. S. Rodriguez, B. Gomez-Martin, *Infrared Phys. Technol.* **2018**, 93, 59.
- [12] G. Kastberger, R. Stachl, *Behav. Res. Methods* **2003**, 3, 429.
- [13] M. Soroko, K. Howell, *J. Equine Vet. Sci.* **2018**, 60, 90.
- [14] Q. Badosa, L. Manosa, E. Vives, A. Planes, B. Weise, L. Beyer, E. Stern-Taulats, *J. Appl. Phys.* **2023**, 134, 113902.
- [15] C. A. Balaras, A. A. Argiriou, *Energy Build.* **2002**, 34, 171.
- [16] U. Prah, M. Sadl, A. Torello, P. Lheritier, V. Kovacova, H. Urisc, E. Defay, *Small Methods* **2023**, 7, 2300212.
- [17] M. Sadl, U. Prah, V. Kovacova, E. Defay, T. Rojac, A. Lebar, J. Valentincic, H. Ursic, *J. Mater. Chem. C* **2023**, 11, 10058.
- [18] A. Aravindhan, P. Lheritier, A. Torello, U. Prah, Y. Nouchokgwe, A. E. Moul, X. Chevalier, F. D. D. Santos, E. Defay, V. Kovacova, *J. Mater. omics* **2023**, 9, 256.
- [19] E. Barreira, R. Almeida, M. Simoes, *Sensors* **2021**, 21, 1961.
- [20] H. Jo, J. L. King, K. Blomstrand, K. Sridharan, *Int. J. Heat Mass Transfer* **2017**, 115, 1065.
- [21] N. Avdelidis, A. Moropoulou, *Energy Build.* **2002**, 35, 663.
- [22] S. Woods, T. Jung, D. Sears, J. Yu, *Cryogenics* **2014**, 60, 44.
- [23] W. Sabuga, R. Todtenhaupt, *High Temp.-High Pressures* **2001**, 33, 261.
- [24] M. G. D. Duca, J. Tusek, A. Maiorino, L. Fulanovic, A. Bradesko, U. Plaznik, B. Malic, C. Aprea, A. Kitanovski, *J. Appl. Phys.* **2020**, 128, 104102.
- [25] P. Wang, Z. Xie, H. Meng, Z. Hu, In *27th Chinese Control and Decision Conf.*, IEEE, Qingdao, China **2015**, pp. 6197–6200.
- [26] Z. Ahcin, S. Dall'Olio, A. Zerovnik, U. Z. Baskovic, L. Porenta, P. Kabirifar, J. Cerar, S. Zupan, M. Brojan, J. Klemenc, J. Tusek, *Joule* **2022**, 6, 2338.
- [27] J. Chen, Y. Zhou, Q. Nan, Y. Sun, Z. Ye, Z. Wang, *Appl. Surf. Sci.* **2007**, 253, 9154.
- [28] Y. Gao, G. Y. Tian, *Sens. Actuators, A* **2018**, 270, 8.
- [29] E. Vives, S. Burrows, R. Edwards, S. Dixon, L. Manosa, A. Planes, R. Romero, *Appl. Phys. Lett.* **2011**, 98, 011902.
- [30] R. Faye, T. Usui, A. Torello, B. Dkhil, X. Moya, N. D. Mathur, S. Hirose, E. Defay, *J. Alloys Compd.* **2020**, 834, 155042.
- [31] K. Xie, J. Housseini, P. M. Resende, F. L. Goupil, J.-D. Isasa, S. Tence-Girault, G. Fleury, H. Kellay, G. Hadziionnou, *Adv. Funct. Matter.* **2024**, 34, 2411397.
- [32] A. Kitanovski, *Adv. Energy Mater.* **2020**, 10, 1903741.
- [33] (Eds: T. Correia, Q. Zhang), *Electrocaloric Materials*, Springer Berlin, Heidelberg, Germany **2014**.
- [34] A. Kitanovski, J. Tusek, U. Tomc, U. Plaznik, M. Ozbolt, A. Poredos, *Magnetocaloric Energy Conversion*, Springer Cham, Cham, Switzerland, **2015**, <https://doi.org/10.1007/978-3-319-08741-2>.
- [35] J. Y. Law, L. M. Moreno-Ramirez, A. Diaz-Garcia, V. Franco, *J. Appl. Phys.* **2023**, 133, 040909.
- [36] V. Franco, J. S. Blasquez, J. J. Ipus, J. Y. Law, L. M. Moreno-Ramirez, A. Conde, *Prog. Mater. Sci.* **2018**, 93, 112.
- [37] N. Zeggai, B. Dkhil, M. LoBlue, M. Almanza, *Appl. Phys. Lett.* **2023**, 122, 081903.
- [38] F. L. Goupil, A. Berenov, A.-K. Azelsson, M. Valant, N. M. Alford, *J. Appl. Phys.* **2012**, 111, 124109.
- [39] K. Klinar, A. Kitanovski, *Renew. Sustain. Energy Rev.* **2020**, 118, 109571.
- [40] T. Swoboda, K. Klinar, A. S. Yalamarthy, A. Kitanovski, M. M. Rojo, *Adv. Electron. Mater.* **2021**, 7, 2000625.
- [41] L. Manosa, A. Planes, *Adv. Mater.* **2017**, 29, 1603607.
- [42] M. J. Pereira, T. Santos, R. Corriea, J. S. Amaral, V. S. Amaral, S. Fabbri, F. Albertini, *J. Phys. Mater.* **2023**, 6, 024002.
- [43] K. Wang, Y. Ouyang, Y. Shen, Y. Zhang, M. Zhang, J. Liu, *J. Mater. Sci.* **2021**, 56, 2332.
- [44] M. Sanilialp, V. V. Shvartsman, R. Faye, M. O. Karabasov, C. Molin, S. Gebhardt, E. Defay, D. C. Lupascu, *Rev. Sci. Instrum.* **2018**, 89, 034903.
- [45] H. Ossmer, F. Lambrecht, M. Gultig, C. Chluba, E. Quandt, M. Kohl, *Acta Mater.* **2014**, 81, 9.
- [46] T. Hirai, R. Iguchi, A. Miura, K.-i. Uchida, *Adv. Funct. Mater.* **2022**, 32, 2201116.
- [47] L. Ianniciello, M. Romanini, L. Manosa, A. Planes, K. Engelbrecht, E. Vives, *Appl. Phys. Lett.* **2020**, 116, 1839011.
- [48] M. A. S. Arian, T. Balkan, *J. Rob. Syst.* **2000**, 17, 479.
- [49] S. Krimi, J. Klier, J. Jonscheit, G. v. Freymann, R. Urbansky, R. Beigang, *Appl. Phys. Lett.* **2016**, 109, 021105.

- [50] I. Mendoza, D. Drury, S. Koumlis, J. Ivy, G. Brennecke, L. Lamberson, *J. Am. Ceram. Soc.* **2022**, *105*, 3116.
- [51] I. Mendoza, D. Drury, A. Matejunas, J. Ivy, S. Koumlis, P. Jewell, G. Brennecke, L. Lamberson, *Eng. Fract. Mech.* **2021**, *247*, 107669.
- [52] U. Tomc, S. Nosa, K. Klinar, A. Kitanovski, *J. Adv. Res.* **2023**, *45*, 157.
- [53] K. Klinar, U. Tomc, B. Jelenc, S. Nosa, A. Kitanovski, *Appl. Energy* **2019**, *236*, 1062.
- [54] Vacuumshmelze, Magnetocaloric Materials Calorivac, <https://vacuumshmelze.com/products/advanced-technologies/magnetocaloric-material-calorivac>.
- [55] M. Katter, V. Zellmann, G. W. Reppel, K. Uestuener, *IEEE Trans. Magn.* **2008**, *44*, 3044.
- [56] V. Regis, H. Uršič, *Zenodo* **2025**, <https://doi.org/10.5281/zenodo.15681995>.